

OTFS Modulation with Phase Noise in mmWave Communications

G. D. Surabhi, M. Kollengode Ramachandran, and A. Chockalingam
Department of ECE, Indian Institute of Science, Bangalore 560012

Abstract—Orthogonal time frequency space modulation (OTFS) modulation is a 2-dimensional modulation technique designed in delay-Doppler domain, suited for doubly dispersive wireless channels. OTFS modulation has been shown to achieve superior error performance compared to the conventional multicarrier systems. In this paper, we investigate the effect of phase noise on the performance of OTFS modulation in mmWave communications, where oscillator phase noise and Doppler shifts are typically high. Towards this, we first develop a vectorized formulation of the input-output relation for OTFS modulation (with OFDM as the inner core) in the delay-Doppler domain, incorporating oscillator phase noise in the effective channel. Using a message passing based signal detection algorithm, we show that OTFS is more robust to oscillator phase noise than OFDM in high Doppler mmWave channels. At an SNR for 14 dB, OTFS achieves two to three order better BER performance compared to OFDM in the presence of oscillator phase noise in a 28 GHz system.

keywords: OTFS modulation, OFDM, delay-Doppler domain, oscillator phase noise, mmWave communication.

I. INTRODUCTION

The demand for high data rates and the availability of huge amount of spectrum in mmWave frequency bands have motivated the design of high throughput wireless systems that operate at mmWave frequencies [1],[2]. However, there are several challenges associated with mmWave communication systems that need to be addressed. The high carrier frequencies used in mmWave systems cause higher Doppler shifts even in low/medium mobility scenarios, making them vulnerable to mobility. Also, higher phase noise associated with high frequency oscillators used in mmWave systems are considered detrimental. Conventional multicarrier modulation techniques like OFDM are primarily designed to mitigate the effect of inter-symbol interference (ISI). The performance of these multicarrier systems depends significantly on the orthogonality of the subcarriers. However, Doppler shift and phase noise effects perturb the orthogonality of subcarriers in these systems, leading to inter-carrier interference (ICI) that results in performance degradation.

Orthogonal time frequency space (OTFS) modulation is a recently proposed modulation scheme, designed in delay-Doppler domain, suited for high Doppler fading channels [3]-[12]. OTFS modulation uses a series of transformations which convert a rapidly time-varying fading channel into an almost invariant channel in the delay-Doppler domain such

that all symbols in a transmission frame experience nearly constant channel gain. This relatively constant channel gain experienced by all the symbols in an OTFS transmission frame can greatly simplify the design of equalizer and reduce the overhead on the channel estimation in rapidly time-varying channels. The transformations used by the OTFS modulation spread the information symbols in the delay-Doppler across the entire time-frequency plane, thereby resulting in superior performance compared to the conventional OFDM systems. OTFS has been shown to achieve significantly better bit error performance compared to OFDM for vehicle speeds ranging from 30 km/h to 500 km/h in 4 GHz band [4],[5]. OTFS operation in mmWave frequency bands has been studied in [6]. Low-complexity signal detectors have been proposed for OTFS signal detection in [7],[8]. Signal detection and channel estimation aspects of OTFS in multiple-input-multiple-output (MIMO) setting have been considered in [9]. The diversity achieved by OTFS has been analyzed in [10]. It has been suggested in [4] that OTFS modulation can be implemented by adding pre- and post- processing blocks to conventional multicarrier modulation systems such as OFDM. Design of OFDM based OTFS systems have been discussed in [11],[12].

This paper addresses the effect of oscillator phase noise on the performance of mmWave OTFS systems, *which has not been reported before*. Towards this, we first develop a vectorized formulation for OFDM based OTFS modulation, which is modular and hence allows us to incorporate the oscillator phase noise in the system model in a structured manner. An RF carrier frequency of 28 GHz with oscillator phase noise characteristics in 3GPP standards [13],[14],[15] is considered. Employing a low-complexity message passing based signal detection algorithm operating on the OFDM based OTFS system model, we investigate the bit error performance in the presence of oscillator phase noise. Our simulation results show that OTFS is more robust to phase noise effects compared to OFDM under various Doppler shifts.

The rest of the paper is organized as follows. The vectorized formulation for OFDM based OTFS modulation which incorporates the oscillator phase noise effects is presented in Sec. II. Message passing based signal detection for the considered system model is presented in Sec. III. Simulation results and discussions on the performance in the presence of phase noise is presented in Sec. IV. Conclusions are presented in Sec. V.

II. SYSTEM MODEL

In this section, we briefly introduce the OTFS modulation, present the vectorized input-output relation for OTFS realized

This work was supported in part by the J. C. Bose National Fellowship, Department of Science and Technology, Government of India, and the Intel India Faculty Excellence Program.

using pre- and post-processing blocks to OFDM, and incorporate the transmitter and receiver phase noise into the vectorized formulation of the input-output relation.

A. OTFS modulation

The block diagram for OTFS modulation architected over OFDM system is shown in Fig. 1. The inner box in the block diagram is the familiar OFDM system and the outer box that includes the pre- and post-processor is the OTFS scheme that operates in the delay-Doppler domain. At the OTFS transmitter, the information symbols (e.g., QAM symbols) denoted by $x_{\text{DD}}[k, l]$ in the delay-Doppler domain are mapped to the time-frequency (TF) symbols $X_{\text{TF}}[m, n]$ through the 2D inverse symplectic finite Fourier transform (ISFFT) and windowing. This TF signal is then passed through the OFDM modulator. The output of the OFDM modulator is transmitted over the linear time-variant (LTV) channel. At the receiver, the received signal is demodulated using OFDM demodulator to obtain the TF symbols $Y_{\text{TF}}[m, n]$. The TF symbols $Y_{\text{TF}}[m, n]$ thus obtained are mapped back to the delay-Doppler domain symbols $y_{\text{DD}}[k, l]$ using the symplectic finite Fourier transform (SFFT). The series of transformations involved in OTFS modulation transforms a time-varying multipath channel into a slowly varying channel in the delay-Doppler domain.

B. Vectorized formulation for OFDM based OTFS

The information symbols $x_{\text{DD}}[k, l]$, $k = 0, \dots, M-1$, $l = 0, \dots, N-1$ are treated as points on the 2D delay-Doppler grid. The transmitter maps these symbols in the 2D delay-Doppler domain to time-frequency (TF) domain through the inverse symplectic Fourier transform (SFFT⁻¹) operation as

$$X_{\text{TF}}[m, n] = \frac{1}{\sqrt{MN}} \sum_{k=0}^{M-1} \sum_{l=0}^{N-1} x_{\text{DD}}[k, l] e^{-j2\pi(\frac{mk}{M} - \frac{nl}{N})}. \quad (1)$$

Let $\mathbf{X}_{\text{DD}} \in \mathbb{C}^{M \times N}$ denote the matrix with information symbols $x_{\text{DD}}[k, l]$ in delay-Doppler domain and \mathbf{X}_{TF} denote the $M \times N$ matrix with entries $X_{\text{TF}}[m, n]$, $m = 0, \dots, M-1$, $n = 0, \dots, N-1$ in the TF domain. A closer look at (1) reveals that SFFT⁻¹ of \mathbf{X}_{DD} is equivalent to computing M -point discrete Fourier transform (DFT) along the columns of \mathbf{X}_{DD} and N -point inverse discrete Fourier transform (IDFT) along the rows of \mathbf{X}_{DD} . Denoting the M -point DFT matrix by \mathbf{F}_M and N -point IDFT matrix by \mathbf{F}_N^H , (1) can be written as

$$\mathbf{X}_{\text{TF}} = \mathbf{F}_M \mathbf{X}_{\text{DD}} \mathbf{F}_N^H. \quad (2)$$

The matrix operation in (2) can be vectorized as

$$\mathbf{x}_{\text{TF}} = (\mathbf{F}_N^H \otimes \mathbf{F}_M) \mathbf{x}_{\text{DD}}, \quad (3)$$

where $\mathbf{x}_{\text{TF}} = \text{vec}(\mathbf{X}_{\text{TF}})$, $\mathbf{x}_{\text{DD}} = \text{vec}(\mathbf{X}_{\text{DD}})$, and \otimes denotes the Kronecker product operation. The signal vector $\mathbf{x}_{\text{TF}} \in \mathbb{C}^{MN \times 1}$ is then partitioned into N blocks, each of length M , denoted by $\mathbf{x}_{\text{TF}}^{(n)}$, $n = 0, \dots, N-1$. Each block $\mathbf{x}_{\text{TF}}^{(n)}$ of length M is then fed to an OFDM modulator with M subcarriers. The OFDM modulator multiplies each block with an M -point IDFT matrix \mathbf{F}_M^H and adds cyclic prefix (CP) to each block. If L_{cp} denotes the length of the CP used, then the length of

each block after cyclic prefixing will be $L = M + L_{\text{cp}}$. Let $\mathbf{I}_{\text{cp}} = [\mathbf{A}_{\text{cp}}^T \mathbf{I}_M]^T$ denote the $L \times M$ CP insertion matrix, where \mathbf{A}_{cp} is the matrix with last L_{cp} rows of the identity matrix \mathbf{I}_M . These operations are performed on each of the N blocks as

$$\tilde{\mathbf{x}}_{\text{TF}} = (\mathbf{I}_N \otimes \mathbf{I}_{\text{cp}})(\mathbf{I}_N \otimes \mathbf{F}_M^H) \mathbf{x}_{\text{TF}}. \quad (4)$$

The vector $\tilde{\mathbf{x}}_{\text{TF}}$ is then transmitted through the LTV channel, and the received signal vector at the receiver is given by

$$\tilde{\mathbf{y}}_{\text{TF}} = \mathbf{H}_{\text{TV}} \tilde{\mathbf{x}}_{\text{TF}} + \mathbf{w}, \quad (5)$$

where $\mathbf{H}_{\text{TV}} \in \mathbb{C}^{NL \times NL}$ denotes the channel matrix and $\mathbf{w} \sim \mathcal{CN}(\mathbf{0}, \sigma^2 \mathbf{I})$. Assuming that the channel has P propagation paths and denoting the channel gain, delay, and Doppler associated with the i th path by h_i , τ_i , and ν_i , respectively, the entries of \mathbf{H}_{TV} are given by [8],[9]

$$h_{\text{TV}}(\tau, n) = \sum_{i=1}^P h_i e^{j2\pi \nu_i n} \delta(\tau - \tau_i). \quad (6)$$

At the receiver, the received vector is partitioned into N blocks of length L and CP is removed from each block. Let $\mathbf{R}_{\text{CP}} = [\mathbf{0}_{M \times L_{\text{cp}}} \mathbf{I}_M]$ denote the $M \times L$ matrix that removes the CP from each OFDM symbol. This is followed by an M -point DFT on each block. Cyclic prefix removal and DFT operations on each of the N blocks can be vectorized as

$$\mathbf{y}_{\text{TF}} = (\mathbf{I}_N \otimes \mathbf{F}_M)(\mathbf{I}_N \otimes \mathbf{R}_{\text{CP}}) \tilde{\mathbf{y}}_{\text{TF}}. \quad (7)$$

Now, let \mathbf{Y}_{TF} denote the $M \times N$ matrix with entries $Y_{\text{TF}}[m, n]$, $m = 0, \dots, M-1$, $n = 0, \dots, N-1$ in TF domain, such that $\mathbf{y}_{\text{TF}} = \text{vec}(\mathbf{Y}_{\text{TF}})$. An SFFT operation is performed on \mathbf{Y}_{TF} that maps the points $Y_{\text{TF}}[m, n]$ in TF domain to points in delay-Doppler domain, denoted by $y_{\text{DD}}[k, l]$, given by

$$y_{\text{DD}}[k, l] = \sum_{n=0}^{N-1} \sum_{m=0}^{M-1} Y_{\text{TF}}[m, n] e^{j2\pi(\frac{mk}{M} - \frac{nl}{N})}. \quad (8)$$

The SFFT of \mathbf{Y}_{TF} is equivalent to computing N -point DFT along the rows of \mathbf{Y}_{TF} and M -point IDFT along the columns of \mathbf{Y}_{TF} . Hence, (8) can be written as

$$\mathbf{Y}_{\text{DD}} = \mathbf{F}_M^H \mathbf{Y}_{\text{TF}} \mathbf{F}_N. \quad (9)$$

With $\mathbf{y}_{\text{DD}} = \text{vec}(\mathbf{Y}_{\text{DD}})$, (9) can be vectorized as

$$\mathbf{y}_{\text{DD}} = (\mathbf{F}_N \otimes \mathbf{F}_M^H) \mathbf{y}_{\text{TF}}. \quad (10)$$

Using (3) to (7) in (10), the end-to-end input-output system model of the OFDM based OTFS system is given by

$$\mathbf{y}_{\text{DD}} = (\mathbf{F}_N \otimes \mathbf{F}_M^H)(\mathbf{I}_N \otimes \mathbf{F}_M)(\mathbf{I}_N \otimes \mathbf{R}_{\text{cp}}) \mathbf{H}_{\text{TV}} (\mathbf{I}_N \otimes \mathbf{I}_{\text{cp}})(\mathbf{I}_N \otimes \mathbf{F}_M^H)(\mathbf{F}_N^H \otimes \mathbf{F}_M) \mathbf{x}_{\text{DD}} + \hat{\mathbf{w}}. \quad (11)$$

Note that $\hat{\mathbf{w}} = (\mathbf{F}_N \otimes \mathbf{F}_M^H)(\mathbf{I}_N \otimes \mathbf{F}_M)(\mathbf{I}_N \otimes \mathbf{R}_{\text{cp}}) \mathbf{w}$ has the same statistics as \mathbf{w} . From (11), the effective channel matrix in the delay-Doppler domain is given by

$$\mathbf{H}_{\text{DD}} = (\mathbf{F}_N \otimes \mathbf{F}_M^H)(\mathbf{I}_N \otimes \mathbf{F}_M)(\mathbf{I}_N \otimes \mathbf{R}_{\text{cp}}) \mathbf{H}_{\text{TV}} (\mathbf{I}_N \otimes \mathbf{I}_{\text{cp}})(\mathbf{I}_N \otimes \mathbf{F}_M^H)(\mathbf{F}_N^H \otimes \mathbf{F}_M). \quad (12)$$

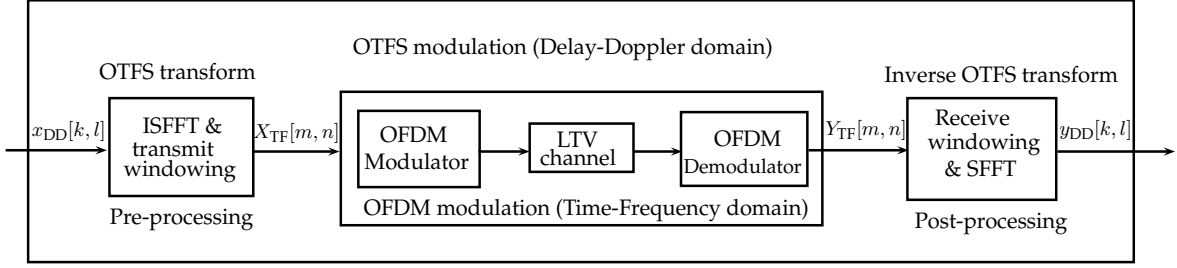


Fig. 1: OFDM based OTFS modulation scheme.

If \mathbf{A} , \mathbf{B} , \mathbf{C} , \mathbf{D} are square matrices, then $(\mathbf{A} \otimes \mathbf{B})(\mathbf{C} \otimes \mathbf{D}) = (\mathbf{AC} \otimes \mathbf{BD})$. Using this property, (12) can be simplified as

$$\mathbf{H}_{DD} = (\mathbf{F}_N \otimes \mathbf{R}_{cp}) \mathbf{H}_{TV} (\mathbf{F}_N^H \otimes \mathbf{I}_{cp}). \quad (13)$$

The input-output relation in (11) can then be expressed as

$$\mathbf{y}_{DD} = \mathbf{H}_{DD} \mathbf{x}_{DD} + \hat{\mathbf{w}}, \quad (14)$$

where $\mathbf{x}_{DD} = \text{vec}(\mathbf{X}_{DD})$ and $\mathbf{y}_{DD} = \text{vec}(\mathbf{Y}_{DD})$ denote the input and output signal vectors in delay-Doppler domain, respectively, \mathbf{H}_{DD} denotes the effective channel matrix in delay-Doppler domain, and $\hat{\mathbf{w}}$ is the AWGN vector.

C. OTFS system with phase noise

In this subsection, the oscillator phase noise associated with the transmitter and receiver is incorporated in the end-to-end OTFS system model in (11). The oscillator output with carrier frequency f_c and phase noise process $\theta_{pn}(t)$, $pn \in \{\text{tx}, \text{rx}\}$, at the transmitter (tx) and receiver (rx), can be modeled as [14]

$$s_{pn}(t) = e^{j2\pi f_c t + \theta_{pn}(t)}. \quad (15)$$

In the discrete time equivalent baseband model, the phase noise process for the n th sample time can be written as

$$s_{pn}(n) = e^{j\theta_{pn}(n)}. \quad (16)$$

The received signal in (11), affected by transmitter and receiver phase noise, can then be written in the form

$$\tilde{\mathbf{y}}_{DD} = (\mathbf{F}_N \otimes \mathbf{F}_M^H)(\mathbf{I}_N \otimes \mathbf{F}_M)(\mathbf{I}_N \otimes \mathbf{R}_{cp}) \Theta_{rx} \mathbf{H}_{TV} \Theta_{tx} (\mathbf{I}_N \otimes \mathbf{I}_{cp})(\mathbf{I}_N \otimes \mathbf{F}_M^H)(\mathbf{F}_N^H \otimes \mathbf{F}_M) \mathbf{x}_{DD} + \hat{\mathbf{w}}. \quad (17)$$

where Θ_{tx} and Θ_{rx} denote the phase noise matrices at the transmitter and the receiver, respectively, and are given by

$$\Theta_{pn} = \text{diag}\{s_{pn}(0), s_{pn}(1), \dots, s_{pn}(NL-1)\}. \quad (18)$$

Thus, from (13) and (17), the effective channel matrix taking into account the transmitter and receiver phase noise matrices Θ_{tx} and Θ_{rx} , can be written in the form

$$\begin{aligned} \tilde{\mathbf{H}}_{DD} &= (\mathbf{F}_N \otimes \mathbf{F}_M^H)(\mathbf{I}_N \otimes \mathbf{F}_M)(\mathbf{I}_N \otimes \mathbf{R}_{cp}) \Theta_{rx} \mathbf{H}_{TV} \Theta_{tx} \\ &\quad (\mathbf{I}_N \otimes \mathbf{I}_{cp})(\mathbf{I}_N \otimes \mathbf{F}_M^H)(\mathbf{F}_N^H \otimes \mathbf{F}_M) \\ &= (\mathbf{F}_N \otimes \mathbf{R}_{cp}) \Theta_{rx} \mathbf{H}_{TV} \Theta_{tx} (\mathbf{F}_N^H \otimes \mathbf{I}_{cp}). \end{aligned} \quad (19)$$

Consequently, as in (14), the received signal with transmitter and receiver oscillator phase noise is given by

$$\tilde{\mathbf{y}}_{DD} = \tilde{\mathbf{H}}_{DD} \mathbf{x}_{DD} + \hat{\mathbf{w}}. \quad (20)$$

III. OTFS SIGNAL DETECTION USING MESSAGE PASSING

In this section, we consider OTFS signal detection with oscillator phase. For this we develop a message passing algorithm for the system model in (20). Dropping the subscripts and tildes in (20) for notational convenience, we write the system model (20) in as $\mathbf{y} = \mathbf{H}\mathbf{x} + \hat{\mathbf{w}}$. This system can be modeled as a sparsely connected factor graph with MN variable nodes corresponding to \mathbf{x} and MN observation nodes corresponding to \mathbf{y} . Let us denote the sets of indices corresponding to the non-zero positions in the b th row and a th column of \mathbf{H} by ζ_b and ζ_a , respectively. Each observation node y_b is connected to the set of variable nodes $\{x_c, c \in \zeta_b\}$, and each variable node x_a is connected to the set of observation nodes $\{y_c, c \in \zeta_a\}$. Denoting the modulation alphabet by \mathbb{A} , the maximum a posteriori (MAP) detection rule for estimating the transmitted signal vector \mathbf{x} is given by

$$\hat{\mathbf{x}} = \underset{\mathbf{x} \in \mathbb{A}^{MN}}{\text{argmax}} \Pr(\mathbf{x}|\mathbf{y}, \mathbf{H}). \quad (21)$$

The joint MAP detection as per (21) has exponential complexity. Hence, we use symbol by symbol MAP rule for $0 \leq a \leq MN-1$ for detection as follows:

$$\begin{aligned} \hat{x}_a &= \underset{a_j \in \mathbb{A}}{\text{argmax}} \Pr(x_a = a_j | \mathbf{y}, \mathbf{H}) \\ &= \underset{a_j \in \mathbb{A}}{\text{argmax}} \frac{1}{|\mathbb{A}|} \Pr(\mathbf{y} | x_a = a_j, \mathbf{H}) \\ &\approx \underset{a_j \in \mathbb{A}}{\text{argmax}} \prod_{c \in \zeta_a} \Pr(y_c | x_a = a_j, \mathbf{H}). \end{aligned}$$

The transmitted symbols are assumed to be equally likely and the components of \mathbf{y} are nearly independent for a given x_a due to the sparsity in \mathbf{H} . The above detection problem can be solved using message passing. The message that is passed from the variable node x_a , for each $a = \{0, 1, \dots, MN-1\}$, to the observation node y_b for $b \in \zeta_a$, is the pmf denoted by $\mathbf{p}_{ab} = \{p_{ab}(a_j) | a_j \in \mathbb{A}\}$ of the symbols in the alphabet \mathbb{A} . The steps involved in the message passing detection are:

- 1: **Inputs:** \mathbf{y} , \mathbf{H} , N_{\max} : maximum number of iterations.
- 2: **Initialization:** Iteration index $t = 0$, pmf $\mathbf{p}_{ab}^{(0)} = 1/|\mathbb{A}| \forall a \in \{0, 1, \dots, MN-1\}$ and $b \in \zeta_a$.
- 3: **Messages from y_b to x_a :** The message passed from y_b to x_a is a Gaussian pdf which can be computed from

Parameter	Value
Carrier frequency (GHz)	28
Bandwidth (MHz)	10
Subcarrier spacing, Δf (kHz)	78.125
Frame size (M, N)	(128,64)
Modulation	BPSK
No. of taps, P	5
Delay profile (μ s)	0.3, 1, 1.7, 2.4, 3.1
Doppler profile (Hz)	0, -400, 400, -1220, 1220

TABLE I: System parameters.

$$y_b = x_a H_{b,a} + \underbrace{\sum_{c \in \zeta_b, c \neq a} x_c H_{b,c}}_{I_{ba}} + \hat{w}_b. \quad (22)$$

The interference plus noise term I_{ba} is approximated as a Gaussian r.v with mean and variance given by

$$\begin{aligned} \mu_{ba}^{(t)} &= \mathbb{E}[I_{ba}] = \sum_{c \in \zeta_b, c \neq a} \sum_{j=1}^{|\mathbb{A}|} p_{cb}^{(t)}(a_j) a_j H_{b,c}, \\ (\sigma_{ba}^{(t)})^2 &= \sum_{c \in \zeta_b, c \neq a} \left(\sum_{j=1}^{|\mathbb{A}|} p_{cb}^{(t)}(a_j) |a_j|^2 |H_{b,c}|^2 - \left| \sum_{j=1}^{|\mathbb{A}|} p_{cb}^{(t)}(a_j) a_j H_{b,c} \right|^2 \right) + \sigma^2. \end{aligned} \quad (23)$$

- 4: **Messages from x_a to y_b :** Messages passed from variable nodes x_a to observation nodes y_b is the pmf vector $\mathbf{p}_{ab}^{(t+1)}$ with the entries given by

$$p_{ab}^{(t+1)} = \Delta p_{ab}^{(t)}(a_j) + (1 - \Delta) p_{ab}^{(t-1)}(a_j), \quad (24)$$

where $\Delta \in (0, 1]$ is the damping factor for improving convergence rate, and

$$p_{ab}^{(t)} \propto \prod_{c \in \zeta_a, c \neq b} \Pr(y_c | x_a = a_j, \mathbf{H}), \quad (25)$$

where

$$\Pr(y_c | x_a = a_j, \mathbf{H}) \propto \exp\left(\frac{-|y_c - \mu_{ca}^{(t)} - H_{c,a} a_j|^2}{\sigma_{c,a}^{2(t)}}\right).$$

- 5: **Stopping criterion:** Repeat steps 3 & 4 till $\max_{a,b,a_j} |p_{ab}^{(t+1)}(a_j) - p_{ab}^{(t)}(a_j)| < \epsilon$ (where ϵ is a small value) or the max. number of iterations, N_{\max} , is reached.
6: **Output:** Output the detected symbol as

$$\hat{x}_a = \underset{a_j \in \mathbb{A}}{\operatorname{argmax}} p_a(a_j), \quad a \in 0, 1, 2, \dots, MN - 1, \quad (26)$$

where

$$p_a(a_j) = \prod_{c \in \zeta_a} \Pr(y_c | x_a = a_j, \mathbf{H}). \quad (27)$$

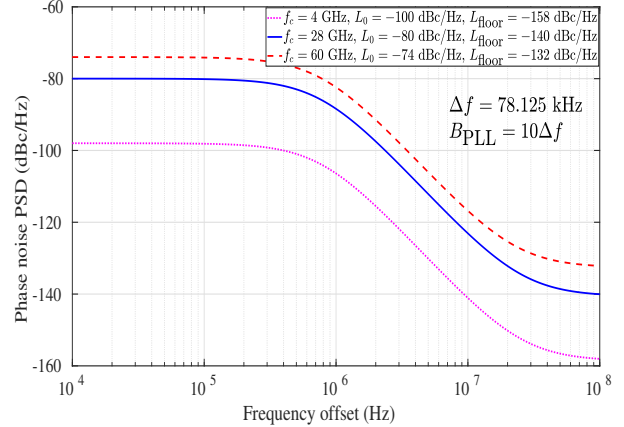


Fig. 2: PSD of oscillator phase noise for various carrier frequencies (4 GHz, 28 GHz, 60 GHz).

IV. RESULTS AND DISCUSSIONS

In this section, we present the performance of OTFS modulation in 28 GHz (mmWave frequency band) in the presence of phase noise and Doppler spread. We evaluated the BER performance of OTFS in the presence of Doppler shift and phase noise using message passing detection. For the same system settings, we also evaluated the performance of OFDM for comparison. The system parameters considered for BER performance evaluation are summarized in Table I. The oscillator phase noise at the transmitter and the receiver is modeled as in [14]. The power spectral density (PSD) of the phase noise is given by [14]

$$L(f_m) = \frac{B_{\text{PLL}}^2 L_0}{B_{\text{PLL}}^2 + f_m^2} + L_{\text{floor}}, \quad (28)$$

where B_{PLL} is the phase locked loop (PLL) -3 dB bandwidth, f_m is the frequency offset from the carrier frequency (f_c), L_0 is the in-band phase noise level in rad^2/Hz , and L_{floor} is the noise floor. It is noted that the oscillator phase noise increases with increased carrier frequencies [15]. This is illustrated in Fig. 2 where the PSD for carrier frequencies of 4 GHz, 28 GHz, and 60 GHz are plotted. These PSDs are plotted using (28) and the parameters obtained from practical oscillators reported in [15] for a base carrier frequency ($f_{c,\text{base}}$) of 30 GHz and shifting its PSD by $20 \log(f_c/f_{c,\text{base}})$ dBc/Hz. The variance of the phase noise samples generated corresponding to the PSDs in Fig. 2 as a function of B_{PLL} (parameterized by n , where $B_{\text{PLL}} = n\Delta f$ and Δf is the subcarrier spacing) is shown in Fig. 3. As we can see, the phase noise variance increases as the PLL bandwidth relative to the subcarrier spacing increases, and this results in increased inter-carrier interference.

We consider a channel model with $P = 5$ paths (taps) and exponential power delay profile. The propagation in mmWave frequencies is dominated by the line-of-sight component, due to which the first tap is considered to follow a Rician fading distribution and the subsequent paths are considered to follow Rayleigh distribution, as in the tapped delay line model (TDL-D) in [13]. The Doppler and delay profiles considered are

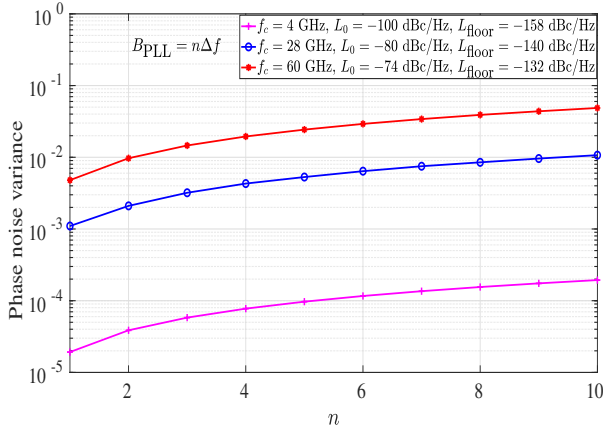


Fig. 3: Variance of the oscillator phase noise as a function of n where $B_{\text{PLL}} = n\Delta f$.

given in Table I. As can be seen, a maximum Doppler shift of 1.22 kHz (which corresponds to a maximum speed of 47 km/h at 28 GHz carrier frequency) is considered. A Rice factor of 13 dB, BPSK modulation, and a damping factor of 0.5 for the message passing algorithm are used.

Figure 4 shows a BER performance comparison between OTFS and OFDM for the system settings described above with a B_{PLL} value of $10\Delta f$ (which corresponds to a high phase noise scenario). From this figure, we observe that the performance of OTFS is superior compared to that of OFDM in the presence of phase noise and Doppler shifts. For example, at a BER of 10^{-3} , the performance of OTFS is better than that of OFDM by about 3 dB. Next, Fig. 5 shows the effect of phase noise alone (i.e., zero Doppler) on the performance of OTFS and OFDM. This figure shows the BER as a function of $B_{\text{PLL}} = n\Delta f$ at a signal-to-noise ratio (SNR) of 14 dB. A two order better BER performance is observed in favor of OTFS compared to OFDM (10^{-5} BER in OTFS vs 10^{-3} BER in OFDM) for $B_{\text{PLL}} = 10\Delta f$. It can also be observed that while OTFS achieves better than 10^{-5} BER for B_{PLL} values from Δf up to $10\Delta f$, OFDM is unable to achieve even 10^{-4} BER at a B_{PLL} of just Δf . It is seen that there is a three order better BER performance in favor of OTFS for $B_{\text{PLL}} = \Delta f$ (i.e., $n = 1$). These results illustrate that OTFS is more resilient to oscillator phase noise in the mmWave band compared to OFDM.

V. CONCLUSIONS

OTFS modulation is a promising multiplexing technique in the delay-Doppler domain, specially suited for high Doppler fading channels. In this work, we presented an end-to-end OFDM based OTFS system model in a vectorized form, which can incorporate the oscillator phase noise at the transmitter and the receiver. Using message passing based signal detection for this system model, we showed that OTFS is more resilient to Doppler shifts and phase noise in the mmWave band.

REFERENCES

[1] T. S. Rappaport, R. W. Heath, Jr., J. N. Murdock, and R. C. Daniels, *Millimeter Wave Wireless Communications*, Prentice Hall, 2014.

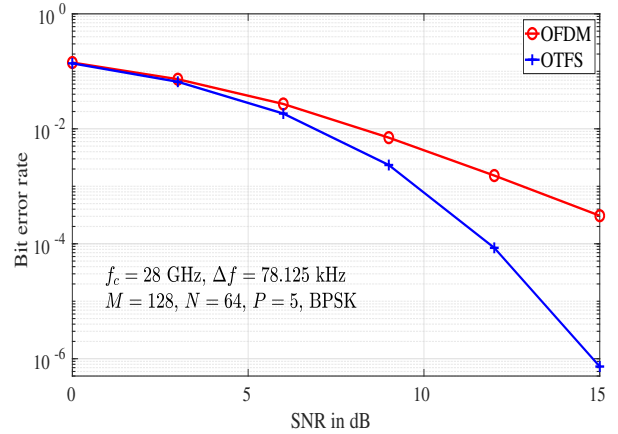


Fig. 4: BER performance comparison between OTFS and OFDM systems with phase noise and Doppler shifts.

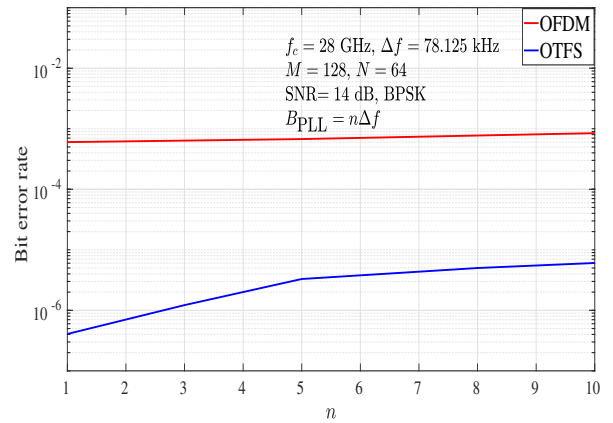


Fig. 5: BER performance comparison between OTFS and OFDM as a function of $B_{\text{PLL}} = n\Delta f$ with zero Doppler.

[2] Y. Niu, Y. Li, D. Jin, L. Su, and A. V. Vasilakos, "A survey of millimeter wave (mmWave) communications for 5G: opportunities and challenges," *Wireless Networks*, vol. 21, no. 8, pp. 2657-2676, Aug. 2015.

[3] R. Hadani, S. Rakib, S. Kons, M. Tsatsanis, A. Monk, C. Ibars, J. Delfeld, Y. Hebron, A. J. Goldsmith, A. F. Molisch, and R. Calderbank, "Orthogonal time frequency space modulation," online: arXiv:1808.00519v1 [cs.IT] 1 Aug 2018.

[4] R. Hadani, A. Monk, "OTFS: A new generation of modulation addressing the challenges of 5G," online: arXiv:1802.02623 [cs.IT] 7 Feb 2018.

[5] R. Hadani, S. Rakib, M. Tsatsanis, A. Monk, A. J. Goldsmith, A. F. Molisch, and R. Calderbank, "Orthogonal time frequency space modulation," *Proc. IEEE WCNC'2017*, pp. 1-7, Mar. 2017.

[6] R. Hadani, S. Rakib, A. F. Molisch, C. Ibars, A. Monk, M. Tsatsanis, J. Delfeld, A. Goldsmith, and R. Calderbank, "Orthogonal time frequency space (OTFS) modulation for millimeter-wave communications systems," in *Proc. IEEE MTT-S Intl. Microwave Symp.*, pp. 681-683, Jun. 2017.

[7] P. Raviteja, K. T. Phan, Y. Hong, and E. Viterbo, "Interference cancellation and iterative detection for orthogonal time frequency space modulation," *IEEE Trans. Wireless Commun.*, vol. 17, no. 10, pp. 6501-6515, Aug. 2018.

[8] K. R. Murali and A. Chockalingam, "On OTFS modulation for high-Doppler fading channels," *Proc. ITA'2018*, San Diego, Feb. 2018.

[9] M. K. Ramachandran and A. Chockalingam, "MIMO-OTFS in high-Doppler fading channels," *Proc. IEEE GLOBECOM'2018*, Dec. 2018. Online: arXiv:1805.02209v1 [cs.IT] 6 May 2018.

[10] G. D. Surabhi, R. M. Augustine, and A. Chockalingam, "On the diversity of OTFS modulation in doubly-dispersive channels," Online: arXiv:1808.07747 [cs.IT] 23 Aug 2018.

[11] L. Li, H. Wei, Y. Huang, Y. Yao, W. Ling, G. Chen, P. Li, and

- Y. Cai, "A simple two-stage equalizer with simplified orthogonal time frequency space modulation over rapidly time-varying channels," online: arXiv:1709.02505v1 [cs.IT] 8 Sep 2017.
- [12] A. Farhang, A. R. Reyhani, L. E. Doyle, and B. Farhang-Boroujeny, "Low complexity modem structure for OFDM-based orthogonal time frequency space modulation," *IEEE Wireless Commun. Lett.*, vol. 7, no. 3, pp. 344 - 347, Jun. 2018.
- [13] *3GPP TR 138.900 V14.2.0: Study on channel model for frequency spectrum above 6 GHz, Release 14 (2017-06)*.
- [14] L. Smaini, *RF Analog Impairments Modeling for Communication Systems Simulation: Application to OFDM-Based Transceivers*, Wiley, 2012.
- [15] *3GPP R1-163984: Discussion on phase noise modeling*, 3GPP TSG RAN WG1 #85, May 2016.